Baseline spectral domain optical coherence tomographic retinal layer features identified by artificial intelligence predict the course of central serous chorioretinopathy

Desideri, L.F.; Anguita, R.; Berger, L.E.; Feenstra, H.M.A.; Scandella, D.; Sznitman, R.; ... ; Zinkernagel, M.S.

OPEN

BASELINE SPECTRAL DOMAIN OPTICAL COHERENCE TOMOGRAPHIC RETINAL LAYER FEATURES IDENTIFIED BY ARTIFICIAL INTELLIGENCE PREDICT THE COURSE OF CENTRAL SEROUS CHORIORETINOPATHY

LORENZO FERRO DESIDERI, MD,*† RODRIGO ANGUITA, MD,*‡ LIESELOTTE E. BERGER, MD,*§ HELENA M. A. FEENSTRA, MD, PHD,¶ DAVIDE SCANDELLA, MSC,** RAPHAEL SZNITMAN, PHD,** CAMIEL J. F. BOON, MD, PHD,¶†† ELON H. C. VAN DIJK, MD, PHD,¶ MARTIN S. ZINKERNAGEL, MD, PHD*†§

Purpose: To identify optical coherence tomography (OCT) features to predict the course of central serous chorioretinopathy (CSC) with an artificial intelligence–based program.

Methods: Multicenter, observational study with a retrospective design. Treatment-naïve patients with acute CSC and chronic CSC were enrolled. Baseline OCTs were examined by an artificial intelligence–developed platform (Discovery OCT Fluid and Biomarker Detector, RetinAI AG, Switzerland). Through this platform, automated retinal layer thicknesses and volumes, including intaretinal and subretinal fluid, and pigment epithelium detachment were measured. Baseline OCT features were compared between acute CSC and chronic CSC patients.

Results: One hundred and sixty eyes of 144 patients with CSC were enrolled, of which 100 had chronic CSC and 60 acute CSC. Retinal layer analysis of baseline OCT scans showed that the inner nuclear layer, the outer nuclear layer, and the photoreceptor–retinal pigmented epithelium complex were significantly thicker at baseline in eyes with acute CSC in comparison with those with chronic CSC ($P < 0.001$). Similarly, choriocapillaris and choroidal stroma and retinal thickness (RT) were thicker in acute CSC than chronic CSC eyes ($P = 0.001$). Volume analysis revealed average greater subretinal fluid volumes in the acute CSC group in comparison with chronic CSC ($P = 0.041$).

Conclusion: Optical coherence tomography features may be helpful to predict the clinical course of CSC. The baseline presence of an increased thickness in the outer retinal layers, choriocapillaris and choroidal stroma, and subretinal fluid volume seems to be associated with acute course of the disease.

RETINA 44:316–323, 2024

Central serous chorioretinopathy (CSC) is a multifactorial chorioretinal disorder, which is characterized by the accumulation of subretinal fluid (SRF) and accounts as the fourth leading, nonsurgical cause of retinopathy after wet age-related macular degeneration, diabetic macular edema, and retinal vein occlusion.[1–3] Central serous chorioretinopathy has been classically subdivided into acute CSC (aCSC) and chronic CSC (cCSC) forms. Although, in aCSC, there is typically a spontaneous resolution of SRF within 6 months from onset, cCSC is characterized by the persistence of visual symptoms (>4–6 months), presence of atrophic retinal pigmented epithelium (RPE) abnormalities, and, in some cases, the formation of choroidal neovascularizations.[4] However, to date, at the first episode of the disease, we are not able to predict the clinical course of this condition. Several previous studies have analyzed demographic and clinical predictive factors that may be related to the clinical course of cCSC.[5–7] Among them, the presence of older age at

presentation, choroidal neovascularization, and the disruption of outer retinal layers by multimodal imaging have been associated with poorer functional outcomes.[5] In a recent study based on optical coherence tomography (OCT), the resolution of SRF in CSC was influenced by the extent of ellipsoid zone damage, SRF height, central macular thickness, and subfoveal choroidal thickness.[7] Recently, artificial intelligence (AI) examining OCT images has been used in patients with CSC, showing promising results in the prediction of disease recurrence and SRF reabsorption.[8–10] In our study, we used an AI-based OCT fluid and biomarker detector to analyze the differences in retinal and choroidal thickness, volumes, and biomarkers between patients with aCSC and cCSC at baseline. The aim of our study was to provide a comprehensive analysis of the OCT biomarkers predictive for the course of the disease and to assess the potential clinical role of AI in the clinical management of CSC.

Materials and Methods

This was a multicenter, retrospective, comparative clinical series of patients with CSC and a minimum follow-up of 1 year conducted at the Department of Ophthalmology, Inselspital University Hospital, Bern (Switzerland), in collaboration with the Department of Ophthalmology, Leiden University Medical Center, Leiden (The Netherlands). Institutional review board approval was obtained from both centers, and all aspects of this retrospective study adhered to the tenets of the Declaration of Helsinki. The diagnosis of CSC was based on clinical history, clinical examination, and multimodal imaging, including OCT, fundus autofluorescence, fluorescein angiography, and indocyanine angiography. In a retrospective analysis, patients with CSC were divided into two groups based on the duration of SRF resolution. Those who exhibited self-resolving SRF within 6 months from the onset of SRF were categorized as patients with aCSC, whereas those with SRF persisting beyond the six-month period were designated as patients with cCSC. Inclusion criteria for patients with cCSC were the presence at fluorescein angiography imaging of multiple RPE leaks in mild and late phases and multifocal areas of RPE alteration on fundus autofluorescence at the last follow-up visit. By contrast, inclusion criteria in the aCSC group were the presence of a single fluorescein leakage site in combination with the absence of other fluorescein angiography abnormalities at baseline and complete resolution of SRF at follow-up. Exclusion criteria were the presence of other macular diseases, previous photodynamic therapy (PDT) or other forms of macular laser, and other interventions, such as antivascular endothelial growth factor injections, history of vitreoretinal surgery, uveitis, glaucoma, optic nerve disease, and medical history positive for systemic disorders potentially affecting the macular status. Patients presenting at baseline with advanced clinical signs of chronic damage at the level of the RPE on the OCT and fundus autofluorescence (hyporeflective/hyperreflective and descending tract autofluorescence patterns[1]) were excluded from this study. Patients with poor image quality and/or artifacts were ruled out from the analysis.

Optical Coherence Tomography Imaging

Optical coherence tomography volumes were acquired from CSC patients with from the databases of the two participating hospitals. The SPECTRALIS SD-OCT imaging system was used (Heidelberg Engineering Inc., Heidelberg, Germany). Optical coherence tomography volumes with a 49-B scan acquisition protocol and a resolution of 496 × 512 pixels per B scan were examined (~125 μm spacing between each scan) centered on the fovea. For each horizontal scan, 9 B scans were averaged. Baseline OCT images were acquired within 30 days from symptoms onset. For both groups (aCSC and cCSC), only baseline OCT images were considered in the analysis.

Quantitative Analysis: Artificial Intelligence–Based Biomarker Optical Coherence Tomography Detector

We used the platform Discovery OCT Biomarker Detector (RetinAI AG, Switzerland) for OCT images analysis. This program was developed through the help of AI, and among its features, it can automatically

From the *Department of Ophthalmology, Inselspital, Bern University Hospital, University of Bern, Bern, Switzerland; †Bern Photographic Reading Center, Inselspital, Bern University Hospital, University of Bern, Bern, Switzerland; ‡Moorfields Eye Hospital NHS Foundation Trust, London; §Department for Bio-Medical Research, University of Bern, Bern, Switzerland; ¶Department of Ophthalmology, Leiden University Medical Center, Leiden, The Netherlands; **ARTORG Research Center Biomedical Engineering Research, University of Bern, Bern, Switzerland; and ††Department of Ophthalmology, Amsterdam University Medical Centers, Amsterdam, The Netherlands.

None of the authors has any financial/conflicting interests to disclose.

Reprint requests: Lorenzo Ferro Desideri, MD, Department of Ophthalmology, and Bern Photographic Reading Center, Inselspital, Bern University Hospital, University of Bern, Freiburgstrasse 18, 3010 Bern, Switzerland; e-mail: lorenzoferrodes@gmail.com

Table 1. Baseline Features of Patients Included in the Study

Demographic and/or Clinical Feature	aCSC n = 60	cCSC n = 100	*P*
Age, years, mean ± SD	48.0 ± 11.2	55.7 ± 10.4	<0.001
Sex, n (%)			0.705
Male	46 (77.6)	79 (79.0)	
Female	14 (22.4)	21 (21.0)	
Laterality, n (%)			0.737
Right	33 (55.0)	49 (49.0)	
Left	27 (45.0)	51 (51.0)	
Ethnicity			0.225
White	55 (91.7)	85 (85.0)	
Asian	0 (0)	2 (2.0)	
Hispanic	2 (3.3)	1 (1.0)	
Middle East–Arabic	3 (5.0)	12 (12.0)	
Baseline SE, D, mean ± SD	+0.56 D ± 1.58	+0.74 D ± 3.1	0.144
Steroid use n (%)	16 (26.6)	17 (17.0)	0.163

D, diopters; SE, Spherical equivalent.

quantify retinal and choroidal thickness, volumes, and biomarkers for each single OCT B scan image.[11,12] In detail, the automated segmentation of retinal and choroidal thicknesses measures the retinal nerve fiber layer, ganglion cell layer and inner plexiform layer (GCL + IPL), inner nuclear layer and outer plexiform layer (INL + OPL), outer nuclear layer (ONL), photoreceptor and RPE layers (PR + RPE) and choriocapillaris with choroidal stroma, and the overall retina thickness (RT). Among the volumes, a quantitative measurement of SRF, intraretinal fluid, and pigment epithelium detachment can be obtained by the program. When an error in automated thickness and/or volumes was present, a manual resegmentation was performed.

Statistical Analysis

Statistical analysis was performed by using Python (3.1) statistics software. The normality of the data was tested using the Shapiro–Wilk test. The difference between sample means of acute and chronic retinal layers and fluids was tested for significance by means of a Welch *t* test. Correlation analysis to measure the strength of the linear relationship between the predictive variables was performed with the Spearman rank correlation coefficient test.

Results

Demographics

We analyzed 160 eyes of 144 patients with CSC, of which 100 eyes (62.5%; n = 90 patients) were diagnosed with cCSC and 60 eyes (34.5%; n = 54 patients) with aCSC. The average age of the study population was 48.0 years (±11.2) in the aCSC group and 55.7 years (±10.4) in the cCSC group ($P < 0.001$). In the aCSC group, 77.6% of the patients were male and 22.3% were female, whereas in the cCSC group, there were 79.0% male patients and 21% female patients ($P = 0.705$). The average spherical equivalent at baseline was +0.56 D (±1.58) in the aCSC group and +0.74 D (±3.1) in the cCSC group, respectively ($P = 0.144$). Baseline demographic and clinical features are summarized in Table 1.

Thickness Analyses

Thickness analysis of baseline OCT scans showed that GCL + IPL was 73.9 ± 5.6 μm and 70.4 ± 8.1 μm in the aCSC and cCSC groups, respectively ($P = 0.002$), whereas retinal nerve fiber layer was

Table 2. Average Retinal and Choroidal Thicknesses Measurements in Patients With aCSC and cCSC

Retinal Layer Thickness (μm)	cCSC	aCSC	*P*
RNFL	41.7 ± 8.5	38.5 μm ± 4.8	0.004
GCL + IPL	70.4 ± 8.1	73.9 ± 5.6	0.002
INL + OPL	55.8 μm ± 5.2	59.7 μm ± 3.8	<0.001
ONL	70.2 μm ± 11.1	79.3 μm ± 7.5	<0.001
PR + RPE	61.8 μm ± 5.9	66.1 μm ± 4.9	<0.001
CC + CS	237.4 μm ± 25.6	251.4 μm ± 22.2	<0.001
RT	320.5 μm ± 41.8	351.4 μm ± 55.4	0.001

CC + CS, choriocapillaris and choroidal stroma; RNFL, retinal nerve fiber layer; RT, retina thickness.

significantly reduced in aCSC (38.5 μm ± 4.8 in aCSC vs. 41.7 ± 8.5 in cCSC, respectively, P = 0.004). The INL + OPL, ONL, and PR + RPE thicknesses were significantly increased at baseline in eyes with aCSC in comparison with those with cCSC (59.7 μm ± 3.8 vs. 55.8 μm ± 5.2, 79.3 μm ± 7.5 vs. 70.2 μm ± 11.1, 66.1 μm ± 4.9 vs. 61.8 μm ± 5.9, respectively, $P < 0.001$). Similarly, choriocapillaris + choroidal stroma and RT were referred to be significantly thicker in aCSC eyes than in cCSC (251.4 μm ± 22.2 vs. 237.4 μm ± 25.6, $P < 0.001$, and 351.4 μm ± 55.4 vs. 320.5 μm ± 41.8, respectively, P = 0.001) (Table 2) (Figure 1).

Retinal Fluids and Volumes

Volume analysis showed that the mean SRF volume was greater in aCSC in comparison with cCSC (1,068.6 nL ± 1,572.2 vs. 571.3 nL ± 1,002.9, respectively, P = 0.041); however, no significant differences were found regarding the average pigment epithelium detachment volume (15.3 nL ± 42.1 vs. 22.9 nL ± 49.9, P = 0.1778) and the average intraretinal fluid (0.1 nL ± 0.4 vs. 2.4 nL ± 15.8, P = 0.1018) in the aCSC and cCSC groups, respectively (Table 3) (Figures 2 and 3).

Correlation analysis (Spearman rank correlation coefficient) showed that there was no significant association between SRF and retinal layer thicknesses, including RT (P = 0.120), INL + OPL (P = 0.233), ONL (P = 0.163), PR + RPE (P = 0.370), and retinal nerve fiber layer (P = 0.172), but there was a significant association between SRF and GCL + IPL thickness (P = 0.019).

Discussion

In this large, multicenter, retrospective study, we analyzed the presence of imaging biomarkers

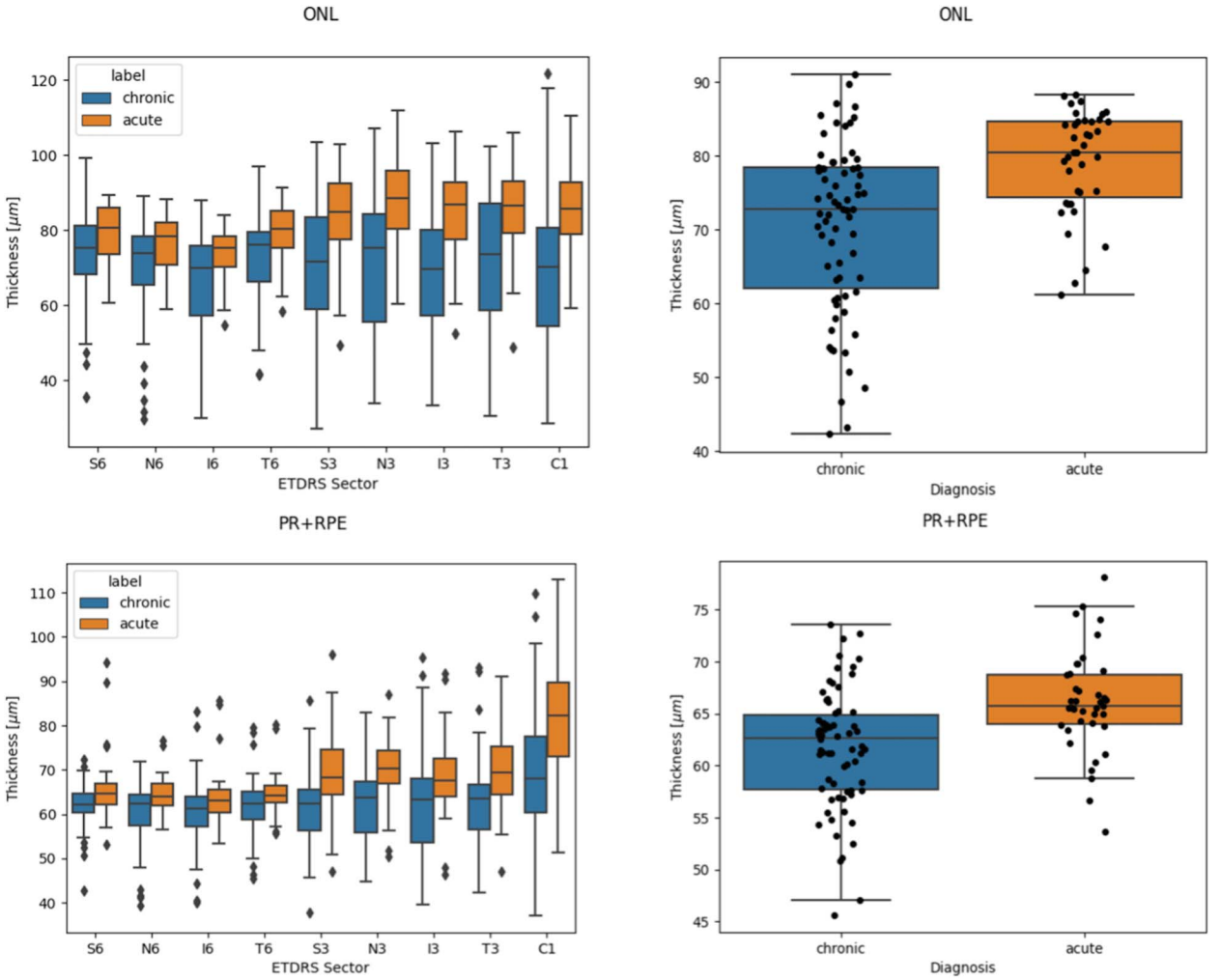

Fig. 1. ONL and PR + RPE thicknesses in aCSC and cCSC groups.

Table 3. Average Retinal Volumes Measurements in Patients With aCSC and cCSC

Retinal Volumes and Fluids (nL)	cCSC	aCSC	*P*
IRF	0.1 nL ± 0.4	2.4 nL ± 15.8	0.1018
SRF	571.3 nL ± 1,002.9	1,068.6 nL ± 1,572.2	0.041
PED	15.3 nL ± 42.1	22.9 nL ± 49.9	0.1778

IRF, intraretinal fluid; PED, pigment epithelium detachment.

associated with the two clinical forms of CSC (aCSC vs. cCSC) using an AI-based biomarker detector. We found the evidence of an increased thickness in both the outer retinal layers (ONL, PR, and RPE layer) and inner retinal layers (INL and GCL) in patients with aCSC as compared with those with cCSC at baseline. We have also found a significantly increased SRF at baseline in patients with aCSC in comparison with cCSC. The importance of finding distinctive imaging biomarkers for clinical disease entity lies in the possibility of identifying the clinical features associated with persistent CSC episodes, in which treatment is necessary to prevent extensive and irreversible visual impairment.[5] This contrasts with aCSC, in which the visual function, color discrimination, contrast, and retinal sensitivity are often largely preserved after spontaneous resolution, which generally occurs within 3 to 4 months after onset, and the role of treatment remains debated.[4] The current gold standard for treating patients with cCSC is half-dose PDT, which has been shown to be superior to the other treatment options, such as high-density subthreshold micropulse laser and oral mineralocorticoid antagonists, such as eplerenone, in large, multicenter clinical trials; however, there is a current worldwide shortage of verteporfin, pushing clinicians to treat with PDT in only the most urgent cases of CSC.[13–16] This situation has exacerbated the importance to distinguish the predictive biomarkers for the clinical course of diseases to facilitate an early diagnosis and management of these patients. Several studies have previously examined the predictive role of retinal biomarkers in CSC.[17–19] In a recent study, Singh et al analyzed the imaging biomarkers in a large sample (n = 231 of 201 patients with CSC) for the prediction of the disease clinical course. They found that the resolution of the disease was correlated with changes in central macular thickness and subfoveal choroidal thickness, whereas modifications in visual acuity at 12 months were associated with SRF height.[7] SRF morphology in CSC was also previously investigated by Subhi et al,[20] who described the SRF shape modification after half-dose PDT and high-density subthreshold micropulse laser. In this study, half-dose PDT was found to be

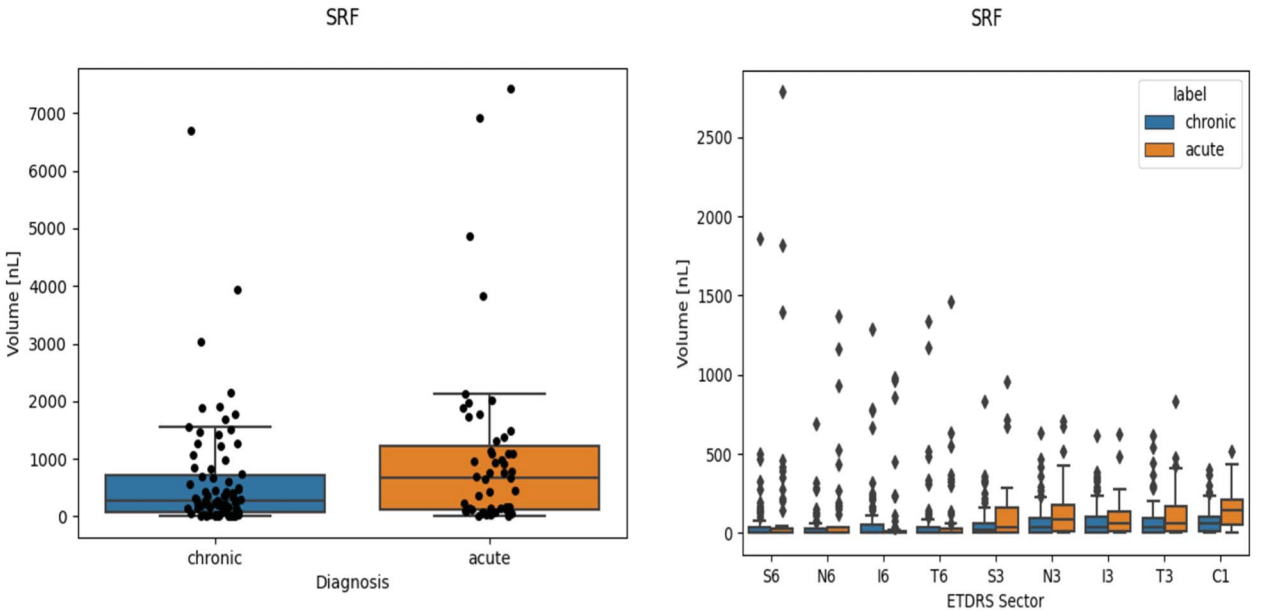

Fig. 2.SRF volume differences between patients with aCSC and cCSC.

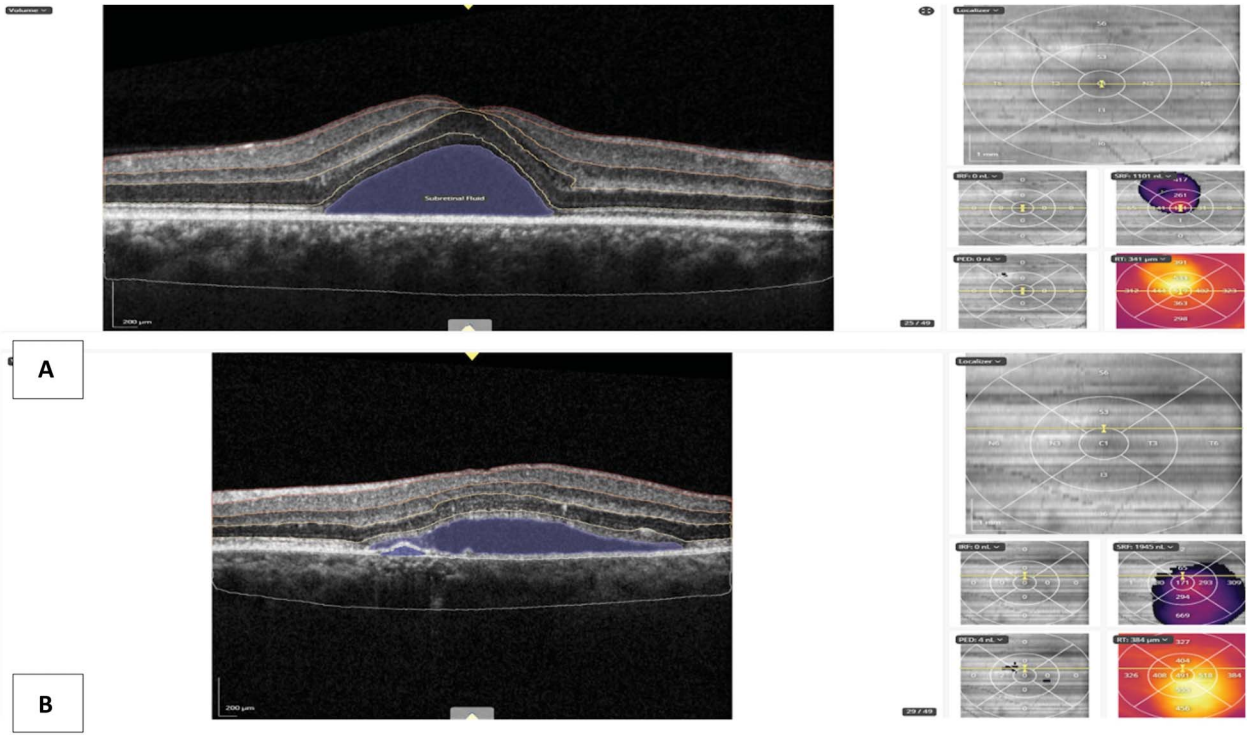

Fig. 3. Different morphology of subretinal fluid in aCSC in comparison with cCSC.

significantly associated with SRF resolution and volume reduction in comparison with high-density subthreshold micropulse laser. However, no predictive role of SRF morphology in treatment response could be extrapolated from that analysis.[20] In our study, our volumetric analysis reported that patients with aCSC had an increased SRF volume at baseline as opposed to cCSC. Feenstra et al described the SRF morphology in patients with cCSC and found that patients presenting the Fuji's sign, characterized by an external limiting membrane displaying a typical concave shape in the context of SRF, were more inclined to have a spontaneous resolution of SRF. Further clinical studies should provide more evidence on the increased volumes of SRF found in acute patients rather than in chronic ones, and we deem that a better understanding of the pathogenic mechanisms involved in the two clinical entities may address us in the possibility to consider SRF as a novel imaging biomarker differentiating aCSC with cCSC forms.

We have also found a significant greater thickness at baseline in the outer retinal layers (ONL and PR + RPE) and inner retinal layers (INL + OPL and GCL) in patients with aCSC in comparison with the cCSC group. The presence of changes in the outer retinal layers in patients with CSC has already been documented in previous studies.[21–23] In a retrospective study on 358 patients with CSC, ONL thinning was found to be proportional to disease duration, with more pronounced differences detected after a disease duration of 6 months.[24] Piccolino et al categorized the eyes of CSC patients with PR layer elongation, which is a stretch of PR length, including the external limiting membrane, the ellipsoid zone, and the interdigitation zone because of SRF in two subgroups: the first group with a preserved anatomy of the outer retinal layers, associated with a better long-term visual prognosis, and a second group, characterized by atrophic changes in the PR layer and poorer visual outcomes.[25] In a recent study, a thinning of the PR layer above the point of focal leakage on fluorescein angiography was found in patients with aCSC as a sign of mild outer retina atrophy. This biomarker was associated with a higher probability of relapsing the episodes of the disease.[21] Our findings are in line with this latter study, in which thinner outer retinal layers in the first episode of cCSC may be predictive regarding the course of the disease. Correlation analysis showed that SRF was influential only for the change of ganglion cell layer + IPL thickness, whereas all the other retinal layers were not subject to variations in thickness due to fluid presence; however, there was no correlation between the extent of SRF and GCL/IPL thinning, which makes a direct causal relationship, for example, through stretching

of the inner retinal layers unlikely. Overall, beside the limitation of the GCL + IPL layer, it seemed that the presence of SRF did not influence our analysis of the retinal thicknesses in the aCSC and cCSC groups. Furthermore, our results showed an increased thickness at baseline in choriocapillaris and choroidal stroma in aCSC in comparison with patients with cCSC. This finding is in line with previous evidence, showing that a thicker choroid is associated with aCSC and may be associated with better functional prognosis.[26–28] In our study, we also found that patients developing cCSC were on average older than those presenting aCSC. This finding is consistent with the evidence provided by previous studies, highlighting the role of older age as an independent risk factor for developing persistent episodes of the disease and poor visual outcome. In this regard, Spaide et al[29] showed that older age was associated with poor visual function, a more pronounced RPE impairment and a higher risk to develop secondary choroidal neovascularization. The potential limitations of our study are the retrospective nature and the relatively small sample size.

In conclusion, OCT biomarkers analysis may help in the prediction of the clinical course of CSC. In particular, the baseline presence of an increased thickness in the outer retinal layers, including INL + OPL, ONL, and PR + RPE; choriocapillaris and choroidal stroma; and SRF volume seems to be associated with aCSC rather than cCSC. Considering the important clinical and therapeutic implications of these findings, further larger-scale studies should provide more evidence in this regard.

Key words: central serous chorioretinoapathy, OCT, OCT biomarkers, AI, disease prediction, acute central serous chorioretinopathy, chronic central serous chorioretinoapathy.

References

1. Kaye R, Chandra S, Sheth J, et al. Central serous chorioretinopathy: an update on risk factors, pathophysiology and imaging modalities. Prog Retin Eye Res 2020;79:100865.
2. van Dijk EH, Nijhoff MF, de Jong EK, et al. Central serous chorioretinopathy in primary hyperaldosteronism. Graefes Arch Clin Exp Ophthalmol 2016;254:2033–2042.
3. Daruich A, Matet A, Dirani A, et al. Central serous chorioretinopathy: recent findings and new physiopathology hypothesis. Prog Retin Eye Res 2015;48:82–118.
4. van Rijssen TJ, van Dijk EHC, Yzer S, et al. Central serous chorioretinopathy: towards an evidence-based treatment guideline. Prog Retin Eye Res 2019;73:100770.
5. Mrejen S, Balaratnasingam C, Kaden TR, et al. Long-term visual outcomes and causes of vision loss in chronic central serous chorioretinopathy. Ophthalmology 2019;126:576–588.
6. Daruich A, Matet A, Marchionno L, et al. Acute central serous chorioretinopathy: factors influencing episode duration. Retina 2017;37:1905–1915.
7. Singh SR, Iovino C, Zur D, et al. Central serous chorioretinopathy imaging biomarkers. Br J Ophthalmol 2022;106:553–558.
8. Xu F, Wan C, Zhao L, et al. Predicting central serous chorioretinopathy recurrence using machine learning. Front Physiol 2021;12:649316.
9. Xu F, Xiang Y, Wan C, et al. Predicting subretinal fluid absorption with machine learning in patients with central serous chorioretinopathy. Ann Transl Med 2021;9:242.
10. Xu F, Wan C, Zhao L, et al. Predicting post-therapeutic visual acuity and OCT images in patients with central serous chorioretinopathy by artificial intelligence. Front Bioeng Biotechnol 2021;9:649221.
11. Habra O, Gallardo M, Meyer Zu Westram T, et al. Evaluation of an artificial intelligence-based detector of sub- and intraretinal fluid on a large set of optical coherence tomography volumes in age-related macular degeneration and diabetic macular edema. Ophthalmologica 2022;245:516–527.
12. Mantel I, Mosinska A, Bergin C, et al. Automated quantification of pathological fluids in neovascular age-related macular degeneration, and its repeatability using deep learning. Transl Vis Sci Technol 2021;10:17.
13. Sirks MJ, van Dijk EHC, Rosenberg N, et al. Clinical impact of the worldwide shortage of verteporfin (Visudyne®) on ophthalmic care. Acta Ophthalmol 2022;100:e1522–e1532.
14. van Dijk EHC, Holtz JK, Sirks MJ, et al. European prevalence of polypoidal choroidal vasculopathy: a systematic review, meta-analysis, and forecasting study. J Clin Med 2022;11:4766.
15. van Dijk EHC, Fauser S, Breukink MB, et al. Half-dose photodynamic therapy versus high-density subthreshold micropulse laser treatment in patients with chronic central serous chorioretinopathy: the PLACE trial. Ophthalmology 2018;125:1547–1555.
16. van Rijssen TJ, van Dijk EHC, Tsonaka R, et al. Half-dose photodynamic therapy versus eplerenone in chronic central serous chorioretinopathy (SPECTRA): a randomized controlled trial. Am J Ophthalmol 2022;233:101–110.
17. Nkrumah G, Paez-Escamilla M, Singh SR, et al. Biomarkers for central serous chorioretinopathy. Ther Adv Ophthalmol 2020;12:2515841420950846.
18. Kiraly P, Smrekar J, Jaki Mekjavic P. Biomarkers predicting central serous chorioretinopathy episode persistence. Eur J Ophthalmol 2022;33(2):11206721221137153.
19. Pfau M, van Dijk EHC, van Rijssen TJ, et al. Estimation of current and post-treatment retinal function in chronic central serous chorioretinopathy using artificial intelligence. Sci Rep 2021;11:20446.
20. Subhi Y, Bjerager J, Boon CJF, van Dijk EHC. Subretinal fluid morphology in chronic central serous chorioretinopathy and its relationship to treatment: a retrospective analysis on PLACE trial data. Acta Ophthalmol 2022;100:89–95.
21. Yu J, Jiang C, Xu G. Correlations between changes in photoreceptor layer and other clinical characteristics in central serous chorioretinopathy. Retina 2019;39:1110–1116.
22. Asano KS, Asaoka R, Asano S, et al. Elongated photoreceptor outer segment length and prognosis of chronic central serous chorioretinopathy. Retina 2020;40:750–757.
23. van Rijssen TJ, Mohabati D, Dijkman G, et al. Correlation between redefined optical coherence tomography parameters and best-corrected visual acuity in non-resolving central serous

chorioretinopathy treated with half-dose photodynamic therapy. PLoS One 2018;13:e0202549.
24. Deng K, Gui Y, Cai Y, et al. Changes in the foveal outer nuclear layer of central serous chorioretinopathy patients over the disease course and their response to photodynamic therapy. Front Med (Lausanne) 2021;8: 824239.
25. Piccolino FC, de la Longrais RR, Ravera G, et al. The foveal photoreceptor layer and visual acuity loss in central serous chorioretinopathy. Am J Ophthalmol 2005;139:87–99.
26. Borrelli E, Zuccaro B, Zucchiatti I, et al. Optical coherence tomography parameters as predictors of treatment response to eplerenone in central serous chorioretinopathy. J Clin Med 2019;8:1271.
27. Ambiya V, Yogi R, Li A, et al. Subfoveal choroidal thickness as a predictor of central serous chorioretinopathy. Eye (Lond). 2016;30:1623–1629.
28. Hamzah F, Shinojima A, Mori R, Yuzawa M. Choroidal thickness measurement by enhanced depth imaging and swept-source optical coherence tomography in central serous chorioretinopathy. BMC Ophthalmol 2014;14:145.
29. Spaide RF, Campeas L, Haas A, et al. Central serous chorioretinopathy in younger and older adults. Ophthalmology 1996; 103:2070–2079.